CHEMISTRY
A EUROPEAN JOURNAL

DOI: 10.1002/chem.200901075

Double Helices with a Controlled Helicity Composed of Biphenol-Derived Phosphoric Acid Diesters

Hidekazu Yamada,[a] Katsuhiro Maeda,*[a, b] and Eiji Yashima*[a]

Since the discovery of the DNA double helix,[1] the developments of artificial double helices have attracted significant attention.[2] Nevertheless, double helices with a controlled helix-sense are quite rare,[2–4] whereas a number of single helical oligomers and polymers have been reported.[5] Metal-directed self-assembly is the most widely used approach to construct double-stranded helices, helicates.[2a–c] Hydrogen-bonding-driven self-assembly is another useful approach to build up supramolecular duplexes.[6] Among them, some aromatic oligoamides were found to fold into double helical structures through hydrogen-bonding along with aromatic–aromatic interactions.[2d–f] Recently, we reported a new modular strategy to build artificial double helical oligomers[3a,c–e] and polymers[3b,f] through amidinium–carboxylate salt bridges, which assist intertwining the two crescent-shaped complementary strands, resulting in the optically active double helices with a controlled helix-sense induced by the chiral groups introduced at the amidine residues.

On the other hand, phosphoric acids are known to form dimers through hydrogen bonds.[7] Moreover, it has been reported that chiral phosphoric acids can function as effective asymmetric organocatalysts.[8] Herein, we report on the design and synthesis of novel artificial double helices by utilizing a specific self-assembly property of biphenol-derived phosphoric acid diesters (Figure 1), whose helical sense can be controlled by chiral substituents introduced onto the phenylene unit as the linker moiety. In addition, chiral amplification during the double helix formation between chiral and achiral strands is also described.

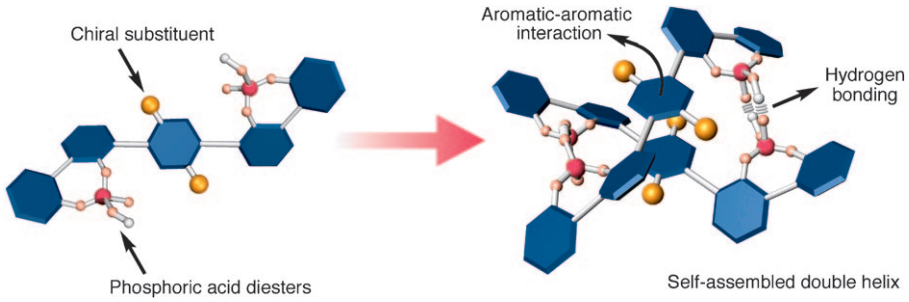

Figure 1. Schematic illustration of self-assembled double helix formation.

Novel chiral ((*S*)-**1**) and achiral (**2**) phosphoric acid diesters were synthesized according to Scheme 1.[9] The dibromide **4** was obtained by the Sonogashira coupling of 2,2′-diacetoxy-3,3′,5,5′-tetrabromobiphenyl with triisopropylsilylacetylene followed by hydrolysis of the ester groups. Lithiation of **4** with *n*BuLi and subsequent quenching with water afforded the monobromide, which was then coupled with tri-*n*-butyl(trimethylsilylethynyl)tin using the Stille coupling reagents to give **7** after the protection of the hydroxy groups. The compound **7** was treated with NaOH and the hydroxy groups were then acetylated to yield **9**. The biphenyl derivative **9** was dimerized by the Sonogashira coupling with (*S*,*S*)-2,5-bis(2-methylbutoxy)-1,4-diiodobenzene[10] as a linker and the dimer product was then treated with phosphoryl chloride after hydrolysis of the acetoxy groups to afford the optically active phosphoric acid diesters (*S*)-**1**.

[a] H. Yamada, Dr. K. Maeda, Prof. E. Yashima
Department of Molecular Design and Engineering
Graduate School of Engineering
Nagoya University
Chikusa-ku, Nagoya 464-8603 (Japan)
Fax: (+81) 52-789-3185
E-mail: maeda@t.kanazawa-u.ac.jp
yashima@apchem.nagoya-u.ac.jp

[b] Dr. K. Maeda
Present address: Graduate School of Natural Science and Technology
Kanazawa University, Kakuma-machi, Kanazawa 920-1192 (Japan)

Supporting information for this article is available on the WWW under http://dx.doi.org/10.1002/chem.200901075.

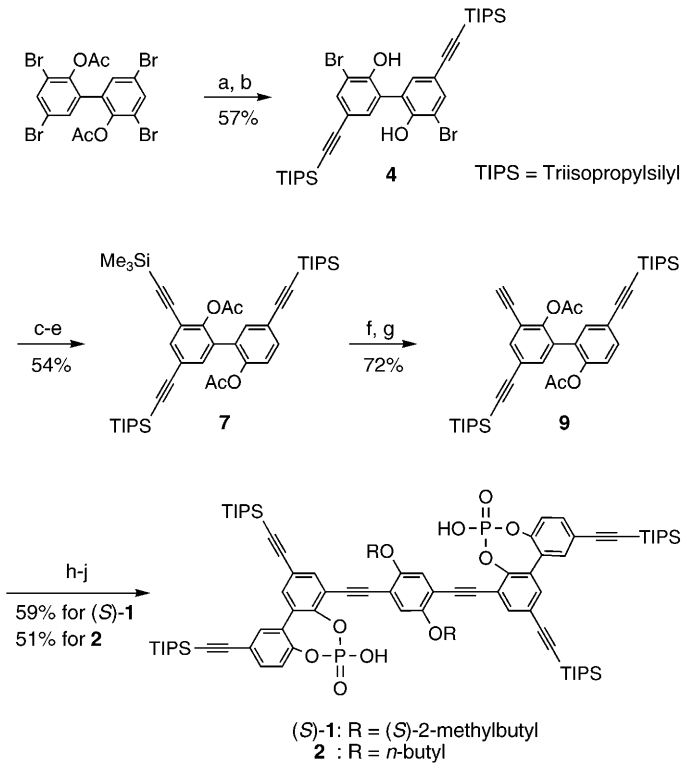

Scheme 1. Syntheses of chiral ((*S*)-**1**) and achiral (**2**) phosphoric acid diesters: a) triisopropylsilylacetylene, $[Pd(PPh_3)_2Cl_2]$, CuI, Et_3N, 30 °C; b) NaOH, MeOH, THF, rt; c) *n*BuLi, THF, H_2O, −78 °C; d) acetyl chloride, pyridine, rt; e) tributyl(trimethylsilylethynyl)tin, $[Pd(PPh_3)_4]$, toluene, reflux; f) K_2CO_3, MeOH, rt; g) acetyl chloride, pyridine, rt; h) (*S*,*S*)-2,5-bis(2-methylbutoxy)-1,4-diiodobenzene for (*S*)-**1**, 2,5-dibutoxy-1,4-diiodobenzene for **2**, $[Pd(PPh_3)_2Cl_2]$, CuI, Et_3N, rt; i) K_2CO_3, MeOH, rt; j) $POCl_3$, pyridine, rt. A detailed version of the scheme including all the intermediate steps and compounds is given in Scheme S1 in the Supporting Information.

The achiral **2** was also synthesized in a similar manner using 2,5-dibutoxy-1,4-diiodobenzene as a linker.[9]

The structure of (*S*)-**1** in solution was first investigated by ^{1}H NMR spectroscopy at 25 °C. In [D_5]pyridine, the ^{1}H NMR signals were sharp, and each signal was assigned to a single strand as its pyridinium salt (Figure 2a). In contrast, these signals became complicated ones in CD_2Cl_2 (Figure 2b). In particular, the signals attributed to the protons for the phenylene linker moieties denoted by f, g, and g′ in Figure 2b were separated into nonequivalent four peaks, respectively, together with additional broad peaks probably due to the diastereomers derived from helicity (see below), and some of them significantly shifted upfield, suggesting a self-assembled formation through hydrogen bonding and aromatic–aromatic interactions in CD_2Cl_2.

2D COSY and ROESY spectra of (*S*)-**1** revealed that the eight peaks (g_1–g_4 and g_1'–g_4' in Figure 2b) were divided into four pairs of the geminal protons bonded to the individual carbon atoms, and the four singlet peaks (f_1–f_4 in Figure 2b) were composed of two pairs of protons exchanging each other (see Figures S4–S10 in the Supporting Information). These observations suggest that the two aromatic rings of the linker moieties are stacked face-to-face, but slightly out of alignment, so that the aromatic linker protons resonated as four singlet peaks. The nonequivalency of these signals is attributed to the formation of a self-assembled homo-duplex of (*S*)-**1**, which was also supported by cold-spray ionization mass spectrometry (CSI-MS) and matrix-assisted laser desorption-ionization time-of-flight mass spectrometry (MALDI-TOF-MS) studies (see Figure S11, S26, and S27b in the Supporting Information).

Repeated attempts failed to produce crystals suitable for X-ray diffraction. Therefore, the energy-minimized structure of the homo-duplex of (*S*)-**1** was calculated based on the hybrid density functional theory (DFT) method at the B3LYP level with the 6-31G* basis set, in which the triisopropylsilylethynyl and (*S*)-2-methylbutoxy substituents of (*S*)-**1** were substituted with hydrogen atoms for simplicity. The calculated structure of the homo-duplex of (*S*)-**1** revealed a double-stranded helical structure (Figure 3), in which the two aromatic rings of the linker moieties overlapped with each other but were slightly out of alignment, and the distance between the two central aromatic rings is about 4 Å. The phosphoric acid residues formed two identical hydrogen bonds, which enabled the two strands to be held together, resulting in a helically twisted double helix (Figure 3). This calculated double-stranded helical structure can explain the results of NMR spectroscopic studies.

Circular dichroism (CD) measurements of (*S*)-**1** were then performed to explore whether (*S*)-**1** formed a preferred-handed homo-double helix in CH_2Cl_2. Compound (*S*)-**1** exhibited an induced circular dichroism (ICD) in the π-conjugated chromophore regions (above 300 nm) (Figure 4a), which is strong evidence that (*S*)-**1** forms a homo-double helix with an excess of either right- or left-handedness. The ICD, however, almost disappeared upon the addition of two equivalents of pyridine at 25 °C; this was accompanied by a change in its absorption spectrum (see Figure S2 in the Supporting Information), resulting from the formation of pyridinium salts with (*S*)-**1** that likely have no regular structure in solution.[11] In addition, the ICD intensity considerably increased on decreasing the temperature and reached an almost constant value at −10 °C (Figure 4a). These ICD changes reversibly took place accompanied by remarkable changes in the absorption spectra. In contrast, the absorption spectrum of an achiral analogue **2** was not temperature dependent (see Figure S13 in the Supporting Information) and its spectral pattern was almost identical to that of (*S*)-**1** at −10 °C (Figure 4a). These results clearly indicate that the optically active substituents introduced on the phenylene linker unit contribute to the bias in an excess of one helical sense, which increased with the decreasing temperature, and the (*S*)-**1** is supposed to adopt an almost one-handed homo-double helical structure at around −10 °C.

This assumption was supported by the variable-temperature ^{1}H NMR measurements of (*S*)-**1** in CD_2Cl_2. As described previously in Figure 2b, the minor peaks (denoted by asterisks in Figure 4b (i) and Figure S1 in the Supporting

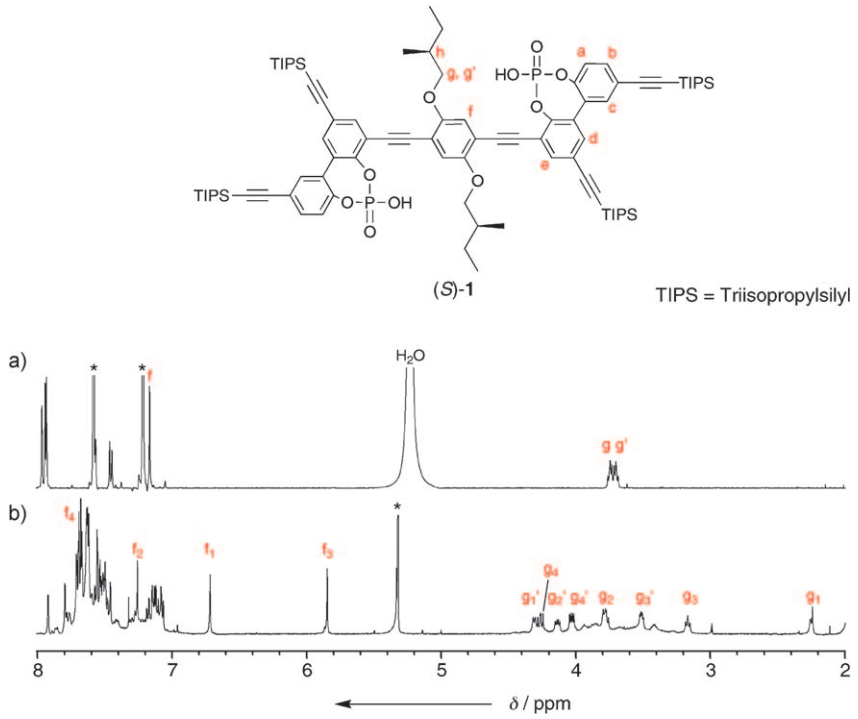

Figure 2. Partial ^{1}H NMR (500 MHz, 25 °C, 6.6 mM) spectra of (*S*)-**1** in [D_5]pyridine (a) and CD_2Cl_2 (b). The asterisks denote the signals for solvents.

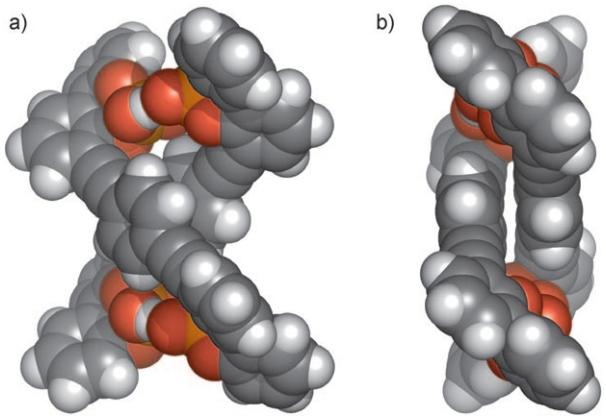

Figure 3. DFT calculated structures (front view (a) and side view (b)) of homo-double helix of (*S*)-**1**. Triisopropylsilylethynyl and (*S*)-2-methylbutoxy groups were substituted with hydrogen atoms for simplicity.

Information), which probably correspond to the opposite diastereomeric homo-double helix, were clearly observed at 35 °C; the intensities of these peaks gradually decreased with the decreasing temperature and the peaks almost disappeared at −10 °C. These changes are also reversible.[12] The analogous achiral strand **2** with no chiral linker units showed a similar ^{1}H NMR spectrum to that of (*S*)-**1** at 25 °C, but no such minor peaks due to diastereomeric helices were observed even at low temperatures (see Figure S12 in the Supporting Information) because **2** self-assembles to form most likely an equal mixture of enantiomeric right- and left-handed double helices (Figure 4b (ii) and Figure S1 in the Supporting Information), resulting in a set of correlated peaks for enantiomeric double helices, as supported by 2D NMR measurements (see Figures S14–S20 in the Supporting Information).[13] On the basis of the changes in the relative peak intensities between the major and minor peaks with temperature, the diastereomeric excess (*de*) values of the homo-double helical (*S*)-**1** were calculated and plotted versus temperature (see Figure S3 in the Supporting Information). We note that the relative changes in the CD intensity at 347 nm and absorbance at 378 nm of (*S*)-**1** (Figure 4a) plotted versus temperature were almost proportional to those in the *de* values with temperature (see Figure S3 in the Supporting Information), indicating that (*S*)-**1** exists as a mixture of diastereomeric right- and left-handed homo-double helices under equilibrium in solution, and one of the helices becomes predominant at low temperatures, which could be monitored by ^{1}H NMR and CD spectroscopies.

Next, we examined if chiral amplification could take place during the hetero-double helix formation between the optically active (*S*)-**1** and achiral **2**, by which a preferred-handed hetero-double helix would be formed. First, the ^{1}H NMR spectrum of an equimolar mixture of (*S*)-**1** and **2** was measured in CD_2Cl_2 to estimate the *de* value of the resulting hetero-double helix of (*S*)-**1**·**2**. However, this proved difficult because of the overlap of the proton resonances of the homo- and hetero-double helices composed of (*S*)-**1** and/or **2**, even at temperatures as low as −10 °C (see Figure S25 in the Supporting Information). The CD spectral changes of mixtures of (*S*)-**1** and **2** were then measured under the conditions of constant [(*S*)-**1** and **2**] with varying [(*S*)-**1**] in CH_2Cl_2 at −10 °C (Figure 5a). The Cotton effect intensities at 347 nm of the mixtures monotonically increased on increasing the mole fraction of (*S*)-**1** (Figure 5b, black bold line), whereas their absorption spectra remained unchanged at −10 °C (Figure 5a).

During the double helix formation, three duplex species, two homo-double helices (*S*)-**1**·(*S*)-**1** and **2**·**2**, and a hetero-double helix (*S*)-**1**·**2** are at equilibrium in solution. Among them, the (*S*)-**1**·(*S*)-**1** and (*S*)-**1**·**2** are optically active, thus contributing to the CD, and the (*S*)-**1**·(*S*)-**1** likely forms a one-handed double helix at −10 °C (approximately 100 % *de*) according to the variable-temperature NMR and CD re-

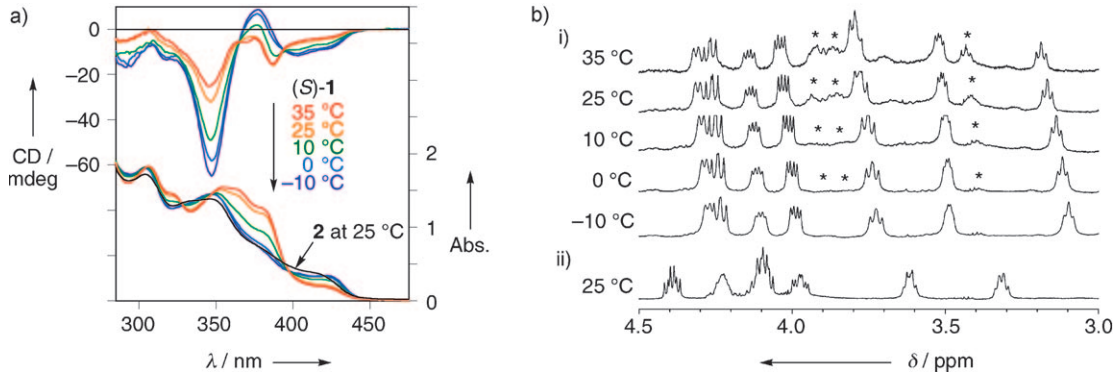

Figure 4. Temperature-dependent spectral changes of (*S*)-**1**. a) CD and absorption spectra (0.60 mM, CH_2Cl_2) of (*S*)-**1** at various temperatures (colored lines). Absorption spectrum (0.60 mM, CH_2Cl_2) of **2** at 25 °C (black line) is also shown. b) Partial ^{1}H NMR (500 MHz, 6.6 mM, CD_2Cl_2) spectra of (*S*)-**1** at various temperatures (i) and **2** at 25 °C (ii). The asterisks denote the signals for the diastereomers.

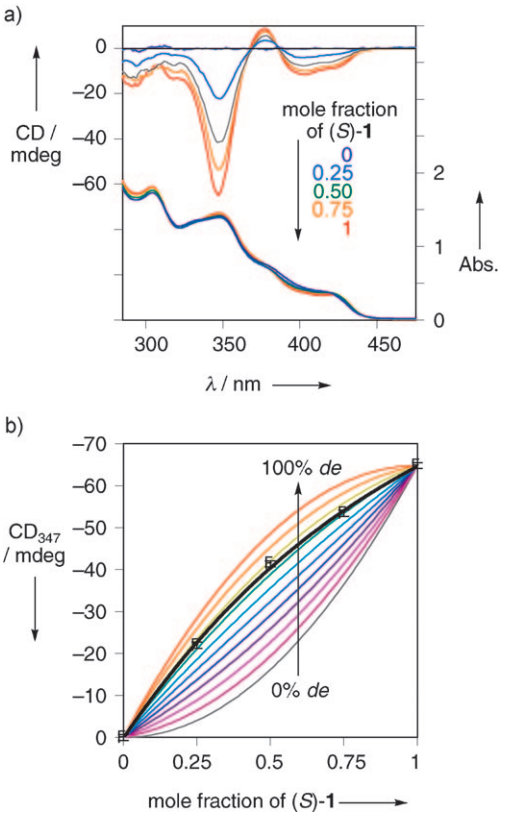

Figure 5. a) CD and absorption spectra (CH_2Cl_2, −10 °C) of (*S*)-**1** with **2**. The total concentration is 0.60 mM and mole fractions of (*S*)-**1** are 0, 0.25, 0.50, 0.75, and 1. b) The approximation curve for the experimental CD intensities at 347 nm (black bold line) and the simulated CD intensity changes on varying the diastereomeric excess (*de*) of (*S*)-**1**·**2** (0–100 % *de* at 10 % intervals) as a function of the mole fraction of (*S*)-**1**.

sults, whereas **2**·**2** is totally optically inactive. We then estimated the excess of one-handedness of the hetero-double helix (*S*)-**1**·**2** on the basis of the following assumptions: 1) The dimerization of (*S*)-**1** and **2** takes place at random, because the MALDI-TOF mass spectrum of an equimolar mixture of (*S*)-**1** and **2** showed that the intensity ratio of the peaks derived from (*S*)-**1**·(*S*)-**1**, (*S*)-**1**·**2**, and **2**·**2** duplexes was approximately 1:2:1 (see Figure S27 in the Supporting Information), 2) (*S*)-**1** and **2** may exist as a homo- or hetero-double helix and free (*S*)-**1** and **2** could be excluded, because their dimerization constants seem to be extremely high over $10^5\,M^{-1}$ (see Figure S23 in the Supporting Information),[14] 3) a hetero-double helix (*S*)-**1**·**2** may have the identical CD pattern to that of (*S*)-**1**·(*S*)-**1** and its maximum CD intensity may be the same as that of the one-handed double helical (*S*)-**1**·(*S*)-**1** at −10 °C, since the absorption spectrum of (*S*)-**1**·(*S*)-**1** at −10 °C, at which the homo-double helix exists in an almost completely one-handedness excess (100 % *de*), was nearly identical to that of the **2**·**2**.

Based on the above assumptions, we simulated the changes in the CD intensity of the mixtures of (*S*)-**1** and **2** at 347, 378, and 403 nm by varying the *de* value of the (*S*)-**1**·**2** hetero-double helix (from 0 to 100 % *de* at 10 % intervals) versus the mole fraction of (*S*)-**1** (Figure 5b and Figure S28 in the Supporting Information). The experimental CD intensity changes fit well with the simulation curves for the *de* values of the hetero-double helix of (*S*)-**1**·**2** (70–80 %). Consequently, chirality is significantly amplified during the hetero-double helix formation between (*S*)-**1** and **2**, leading to an excess of the one-handed hetero-double helix of approximately 70–80 % *de*.

In summary, we have successfully prepared the artificial homo- and hetero-double helices through the assemblies of biphenol-derived phosphoric acid diesters. A bias in the twist sense of the double helices can be achieved by incorporating chiral substituents into the linker unit. Furthermore, a strong chiral amplification was observed during the double helix formation between chiral (*S*)-**1** and achiral **2**. We believe that this novel hydrogen-bond-driven double helix with a controlled helix-sense may provide a new design strategy to develop a variety of discrete supramolecular helical assemblies with a controlled helicity, and novel chiral materials for possible applications in asymmetric catalysis and enantioselective selectors.

Acknowledgements

We thank Dr. Ivan Huc for his invaluable comments and fruitful discussion. We are deeply grateful to Dr. Y. Furusho (Nagoya University) for fruitful discussions. This work was supported in part by Grant-in-Aid for Scientific Research (S) from the Japan Society for the Promotion of Science (JSPS).

Keywords: chiral amplification · chirality · helical structures · self-assembly · supramolecular chemistry

[1] J. D. Watson, F. C. Crick, *Nature* **1953**, *171*, 737–738.
[2] For reviews and selected examples of artificial double helices including helicates, see: a) J.-M. Lehn, *Supramolecular Chemistry*, VCH, Weinheim, **1995**; b) C. Piguet, G. Bernardinelli, G. Hopfgartner, *Chem. Rev.* **1997**, *97*, 2005–2062; c) M. Albrecht, *Chem. Rev.* **2001**, *101*, 3457–3497; d) V. Berl, I. Huc, R. G. Khoury, M. J. Krische, J.-M. Lehn, *Nature* **2000**, *407*, 720–723; e) V. Berl, I. Huc, R. G. Khoury, J.-M. Lehn, *Chem. Eur. J.* **2001**, *7*, 2810–2820; f) I. Huc, *Eur. J. Org. Chem.* **2004**, 17–29.
[3] a) Y. Tanaka, H. Katagiri, Y. Furusho, E. Yashima, *Angew. Chem.* **2005**, *117*, 3935–3938; *Angew. Chem. Int. Ed.* **2005**, *44*, 3867–3870; b) M. Ikeda, Y. Tanaka, T. Hasegawa, Y. Furusho, E. Yashima, *J. Am. Chem. Soc.* **2006**, *128*, 6806–6807; c) Y. Furusho, Y. Tanaka, E. Yashima, *Org. Lett.* **2006**, *8*, 2583–2586; d) Y. Furusho, E. Yashima, *Chem. Rec.* **2007**, *7*, 1–11; e) T. Hasegawa, Y. Furusho, H. Katagiri, E. Yashima, *Angew. Chem.* **2007**, *119*, 5989–5992; *Angew. Chem. Int. Ed.* **2007**, *46*, 5885–5888; f) T. Maeda, Y. Furusho, S.-I. Sakurai, J. Kumaki, K. Okoshi, E. Yashima, *J. Am. Chem. Soc.* **2008**, *130*, 7938–7945.
[4] a) H. Sugiura, Y. Nigorikawa, Y. Saiki, K. Nakamura, M. Yamaguchi, *J. Am. Chem. Soc.* **2004**, *126*, 14858–14864; b) H. Goto, H. Katagiri, Y. Furusho, E. Yashima, *J. Am. Chem. Soc.* **2006**, *128*, 7176–7178.
[5] For reviews on artificial single helical oligomers and polymers, see a) M. M. Green, J.-W. Park, T. Sato, A. Teramoto, S. Lifson, R. L. B. Selinger, J. V. Selinger, *Angew. Chem.* **1999**, *111*, 3328–3345; *Angew. Chem. Int. Ed.* **1999**, *38*, 3138–3154; b) D. J. Hill, M. J. Mio, R. B. Prince, T. S. Hughes, J. S. Moore, *Chem. Rev.* **2001**, *101*, 3893–4011; c) T. Nakano, Y. Okamoto, *Chem. Rev.* **2001**, *101*, 4013–4038; d) J. J. L. M. Cornelissen, A. E. Rowan, R. J. M. Nolte, N. A. J. M. Sommerdijk, *Chem. Rev.* **2001**, *101*, 4039–4070; e) L. Brunsveld, B. J. B. Folmer, E. W. Meijer, R. P. Sijbesma, *Chem. Rev.* **2001**, *101*, 4071–4097; f) M. Fujiki, *Macromol. Rapid Commun.* **2001**, *22*, 539–563; g) E. Yashima, K. Maeda, T. Nishimura, *Chem. Eur. J.* **2004**, *10*, 42–51; h) E. Yashima, K. Maeda, *Macromolecules* **2008**, *41*, 3–12.
[6] a) J. Sánchez-Quesada, C. Steel, P. Prados, J. de Mendoza, *J. Am. Chem. Soc.* **1996**, *118*, 277–278; b) A. P. Bisson, C. A. Hunter, *Chem. Commun.* **1996**, 1723–1724; c) J. L. Sessler, R. Wang, *J. Am. Chem. Soc.* **1996**, *118*, 9808–9809; d) B. Gong, Y. Yan, H. Zeng, E. Skrzypczak-Jankunn, Y. W. Kim, J. Zhu, H. Ickes, *J. Am. Chem. Soc.* **1999**, *121*, 5607–5608; e) B. J. B. Folmer, R. P. Sijbesma, H. Kooijman, A. L. Spek, E. W. Meijer, *J. Am. Chem. Soc.* **1999**, *121*, 9001–9007; f) P. S. Corbin, S. C. Zimmerman, *J. Am. Chem. Soc.* **2000**, *122*, 3779–3780; g) E. A. Archer, N. T. Goldberg, V. Lynch, M. J. Krische, *J. Am. Chem. Soc.* **2000**, *122*, 5006–5007; h) J. S. Nowick, D. M. Chung, K. Maitra, S. Maitra, K. D. Stigers, Y. Sun, *J. Am. Chem. Soc.* **2000**, *122*, 7654–7661; i) G. Schmuck, W. Wienand, *J. Am. Chem. Soc.* **2003**, *125*, 452–459; j) T. Moriuchi, T. Tamura, T. Hirao, *J. Am. Chem. Soc.* **2004**, *126*, 9356–9357.
[7] M. Hojo, H. Hasegawa, Z. Chen, *Bull. Chem. Soc. Jpn.* **1996**, *69*, 2215–2220.
[8] a) T. Akiyama, J. Itoh, K. Yokota, K. Fuchibe, *Angew. Chem.* **2004**, *116*, 1592–1594; *Angew. Chem. Int. Ed.* **2004**, *43*, 1566–1568; b) D. Uraguchi, M. Terada, *J. Am. Chem. Soc.* **2004**, *126*, 5356–5357.
[9] See the Supporting Information for details of the synthesis, structures, and characterization of compounds.
[10] R. Fiesel, U. Scherf, *Acta Polym.* **1998**, *49*, 445–449.
[11] In CH_2Cl_2, an intense split-type ICD was also observed at around 250 nm probably due to the absorption of the biphenol moieties. However, the addition of ethanol resulted in the disappearance of the ICD in the absorption region of the biphenol moieties as well as the π-conjugated chromophore region (see Figure S2 in the Supporting Information). These results indicate that a preferred-handed axially twisted conformation was also induced in the biphenol moieties upon the formation of a homo-double helix with an excess handedness.
[12] There may be another possibility to explain the changes in the absorption, CD, and ^{1}H NMR spectra of (*S*)-**1** as a function of the temperature; that is, formation of a small aggregate for (*S*)-**1** rather than a specific duplex at high temperature, and this possibility could not be completely excluded, although the MS data support the duplex formation.
[13] From the diffusion-ordered ^{1}H NMR spectroscopy (DOSY) measurements for (*S*)-**1** and **2** in CD_2Cl_2 in the presence of the monomeric (*S*)-**11** (see Scheme S1 in the Supporting Information) as the internal standard, the diffusion constants of (*S*)-**1** and **2** were determined to be $D \approx 4.0 \times 10^{-10}\,m^2 s^{-1}$; these values were smaller than that of (*S*)-**11** ($D \approx 6.0 \times 10^{-10}\,m^2 s^{-1}$) (see Figure S21 and S22 in the Supporting Information). These results indicate that (*S*)-**1** and **2** form a similar aggregate, probably a dimer with an almost identical molecular weight in CH_2Cl_2, although their absorption and NMR spectral patterns differ.
[14] The dimerization constant of **2** in CH_2Cl_2 at room temperature was too large ($>10^5\,M^{-1}$) to be determined by absorption spectroscopy (see Figure S23 in the Supporting Information). Therefore, it was estimated by fluorescence spectroscopy to be 5.9×10^6 (see Figure S24 in the Supporting Information).

Received: April 22, 2009
Published online: June 16, 2009

